

RESEARCH NOTE

Anti-ASF Distribution of Fischer–Tropsch Hydrocarbons in Supercritical-Phase Reactions

Noritatsu Tsubaki,^{*,1} Kiyotaka Yoshii,[†] and Kaoru Fujimoto[‡]

^{*}Department of Material Systems and Life Science, School of Engineering, Toyama University, Gofuku, Toyama, 930-8555, Japan; [†]Organic Synthesis Division, Ube R&D, Ube Industries Co., Ube, Yamaguchi, 755-8633, Japan; and [‡]Dean's Office, School of Engineering, University of Kitakyushu, Hibikino, Wakamatsu-ku, Kitakyushu, 808-0135, Japan

Received July 13, 2001; revised January 15, 2002; accepted January 15, 2002

Direct wax synthesis from syngas was implemented by supercritical-phase Fischer–Tropsch synthesis (FTS) reaction. By introducing supercritical-phase *n*-pentane into the reaction, waxy hydrocarbon formation rate was increased significantly while light hydrocarbon formation rate was suppressed effectively. Anti-Anderson–Schultz–Flory distribution of FTS hydrocarbons was realized at lower temperatures, such as 473 K. The intermediate, olefins, readily readsorbed onto the catalyst surface and significantly stimulated the carbon chain-growth process. © 2002 Elsevier Science (USA)

Key Words: Fischer–Tropsch synthesis; wax; cobalt catalyst; chain initiation; readsorption.

INTRODUCTION

Generally, Fischer–Tropsch synthesis (FTS) hydrocarbon formation dependence on carbon chain length is controlled by the Anderson–Schultz–Flory (ASF) distribution law. It is impossible to selectively synthesize parts of hydrocarbons while stopping formation of other parts as FTS proceeds via polymerization of $-\text{CH}_2-$ species (1). Especially it is difficult to synthesize wax efficiently from syngas through FTS by suppressing formation of light hydrocarbons, where wax is formed via light hydrocarbons during the carbon chain-growth process.

Wax synthesis is important in the FTS industry. Furthermore it can be hydrocracked successively to form isoparaffin, where FTS itself mainly produces straight-chain hydrocarbons, including wax (2). To obtain wax in high yield, restriction of ASF distribution should be released.

Significant research has been conducted to investigate the effect of adding light olefins, such as ethylene or propylene, into synthesis gas on the behavior of the FTS reaction (3–10). It has been found that olefins might initiate chains

or become part of a growing chain. Their effect on carbon chain growth was, however, very weak, as the chain-growth probability remained nearly the same. For example, only the formation rate of the C_3 fraction increased in an ethylene-added FTS reaction. Also, a hydroformylation reaction often happened with the addition of these light olefins. The short carbon chain of these light olefins and their high diffusivity in the catalyst inner surface in the gas-phase reaction might severely limit their contribution to carbon chain growth (11, 12).

The present authors introduced small amounts of 1-olefins, such as 1-tetradecene or 1-hexadecene, to FTS in the supercritical phase, finding that the added 1-olefins were transported to the inner surface of the catalyst pellets with the aid of accompanying supercritical fluid, to stimulate wax formation. As the added olefin adsorbed onto metallic sites of FTS catalysts to initiate a new carbon chain-growth process with the intrinsic $-\text{CH}_2-$ from syngas, wax formation was increased effectively and CO conversion was also enhanced in most cases. This phenomenon was not available in gas-phase or liquid-phase reactions (13).

The present report provides findings that anti-ASF distribution was also available without addition of 1-olefins, at lower reaction temperatures, such as 473 K, in supercritical-phase FTS reactions.

EXPERIMENTAL

Two series of cobalt-based catalysts were prepared. A Co/SiO₂ catalyst was prepared by impregnating a cobalt nitrate aqueous solution onto a silica gel (Fuji Davison ID, specific surface area, 127 m²/g; pore volume, 0.69 cm³/g) via the incipient wetness method. The other kind of catalyst was Co–La/SiO₂, where all metal components were simultaneously impregnated onto the same silica gel from their nitrate aqueous solution by the same incipient wetness method. Catalyst precursors were dried in air at 393 K

¹ To whom correspondence should be addressed. Fax: 81-76-445-6846. E-mail: tsubaki@eng.toyama-u.ac.jp.

for 12 h and then calcined in air for 1 h at specific temperatures. Fresh catalysts were treated with flowing hydrogen at 673 K for 12 h *in situ* before use. Catalyst pellets (1 g) the size of 20–40 mesh were mixed with quartz sand (4 g) before loading. Also 2 g of glass beads were loaded upstream from the catalyst bed. A RINT 2400 (Rigaku) X-ray diffractometer instrument with monochromatized $\text{CuK}\alpha$ radiation was used for X-ray diffraction measurement of the reduced catalysts. The Scherrer equation was used to determine the size of the cobalt crystalline. Dispersion of cobalt was determined by static CO chemisorption in a vacuum system and turnover frequency (TOF) was calculated using the data from cobalt dispersion.

The supercritical fluid *n*-pentane (T_c , 470 K, P_c , 33.3 bar) was utilized as the reaction medium. The process flow of the supercritical-phase reaction was similar to that used in our previous work (14). It should be noted that this flow-type reaction apparatus could be used either for the gas-phase reaction or for the liquid-phase reaction (trickle bed) if the accompanying material is changed. Accumulated products, transported by the supercritical fluid into the ice-trap, were analyzed hourly. Supercritical fluid was also employed to extract the residual hydrocarbons in the catalyst bed after the supercritical-phase reaction. As reported before (14), very little product was extracted. Each experiment was conducted for 12 h and the reaction performance generally reached steady state for the second hour after the start. Catalyst deactivation was not observed, partly due to the coexistence of supercritical fluid. Reproducibility of the experiments was recognized.

Gaseous products were analyzed with online gas chromatographs. CO and CO_2 were analyzed using an activated charcoal or molecular sieve column equipped with a thermal conductivity detector. Light hydrocarbons were analyzed using a Porapak-Q column with a flame ionization detector (FID). Hydrocarbons dissolved in the *n*-pentane were analyzed using a Silicone SE-30 column with FID. Capillary columns (OV-1 or OV-1701 bonded) as well as a high-temperature gel permeation chromatograph

(Walters, 860/V2.2) were used for precise analysis of the products.

The standard reaction conditions were P (total) = 45 bar, P ($\text{CO} + \text{H}_2$) = 10 bar, P (*n*-pentane) = 35 bar, $\text{CO}/\text{H}_2 = 1/2$, W/F ($\text{CO} + \text{H}_2$) = 9 g/mol h^{-1} , and $T = 473\text{--}493$ K. Argon was used as an internal standard with a concentration of 3% in the feed gas.

RESULTS

As wax formation is favored at lower temperature, it is necessary to conduct the FTS at lower temperature, while methane formation can be also suppressed. To realize the supercritical-phase FTS reaction conditions at lower reaction temperature, *n*-pentane was selected as the supercritical fluid reaction medium, instead of *n*-hexane (T_c : 507 K; P_c : 29.7 bar) which was often used in our previous experiments (15). All the reactions showed very stable time-on-stream catalyst activity, and temperature variance along the reactor was within 1–2 K.

A lower reaction temperature favored the chain-growth process but CO conversion of the catalyst would be decreased. It is necessary to develop highly active catalysts at lower temperatures. From the FTS theory, large supported metallic crystalline favored carbon chain growth but overall CO conversion was low, as the metal dispersion was not high (16, 17). A supported catalyst with both large metallic surface and large metallic particle size is necessary if TOF is the same. To control metal dispersion, one effective method is adjustment of the calcination temperature. Table 1 shows the calcination temperature effect on a Co–La/SiO₂ catalyst. La addition to a cobalt catalyst was reported to promote the decomposition of the adsorbed CO on cobalt surface (18). It is clear that higher calcination temperatures increased chain-growth probability, and lower calcination temperatures increased CO conversion. Generally, higher reaction temperatures favored high CO conversion but low-chain-growth probability and high methane selectivity. It is indicated that increasing calcination temperatures from 423

TABLE 1
Calcination Temperature Effect on Co–La/SiO₂ Catalysts^a

Reaction temp. (K)	Calcination temp. (K)	CO conv. (%)	CH ₄ sel. (%)	Chain-growth probability (α)	Co particle size from XRD (nm)	Co dispersion (%)	TOF (10^{-2} s^{-1})	Wax sel. ^b (%)
483	723	19.8	4.6	0.93	46.0	2.09	2.87	47.8
493	723	25.8	4.6	0.92	46.0	2.09	3.74	42.9
483	573	23.5	4.7	0.91	42.2	2.28	3.12	38.0
493	573	35.9	4.9	0.90	42.2	2.28	4.77	33.3
483	423	23.5	3.0	0.89	32.9	2.92	2.44	28.9
493	423	49.1	6.0	0.84	32.9	2.92	5.09	12.6

^a Catalyst composition: Co/La/SiO₂ = 25/3/100 (wt.); P (total) = 45 bar; P ($\text{CO} + \text{H}_2$) = 10 bar; P (*n*-pentane) = 35 bar; $\text{CO}/\text{H}_2 = 1/2$; W/F ($\text{CO} + \text{H}_2$) = 9 g/mol h^{-1} .

^b Wax selectivity is the percentage of C20–C45 in C1–C45.

TABLE 2
Calcination Temperature Effect on Co/SiO₂ Catalysts^a

Reaction temp. (K)	Calcination temp. (K)	CO conv. (%)	CH ₄ sel. (%)	Chain-growth probability (α)	Co particle size from XRD (nm)	Co dispersion (%)	TOF (10 ⁻² s ⁻¹)	Wax sel. ^b (%)
483	723	70.1	3.3	0.90	49.4	1.95	7.60	33.3
483	573	76.7	2.4	0.90	44.2	2.18	7.46	33.3
483	423	84.0	2.1	0.89	39.1	2.46	7.24	28.9
473	423	42.9	3.1	0.96	39.1	2.46	3.59	55.8
473 ^c	423	45.0	7.1	0.91	39.1	2.46	3.77	38.0

^a Catalyst composition: Co/SiO₂ = 40/100 (wt.); P (total) = 45 bar; P (CO + H₂) = 10 bar; P (*n*-pentane) = 35 bar; CO/H₂ = 1/2; W/F (CO + H₂) = 9 g/mol h⁻¹.

^b Wax selectivity is the percentage of C₂₀–C₄₅ in C₁–C₄₅.

^c Gas-phase reaction, the same reaction conditions as above except *n*-pentane was replaced by nitrogen.

to 723 K enlarged the size of the cobalt particle from 32.9 to 46.0 nm. The catalyst calcined at 723 K exhibited high-chain-growth probability, such as 0.92 or 0.93, when the reaction temperature was 493 or 483 K. Cobalt dispersion increased with a decreased calcination temperature. TOF did not show a regular changing trend, due to the influence of La addition.

Table 2 compares the reaction behavior of Co/SiO₂ catalysts calcined at different temperatures. The loading amount of cobalt was 28.6 wt% (Co/SiO₂ = 40/100). It is clear that CO conversion was higher for the low-temperature-calcined catalyst. Cobalt dispersion increased with a decreased calcination temperature. TOF showed a typical changing trend. For the monometallic catalyst here, the larger cobalt crystalline exhibited a higher TOF (17). When the reaction temperature was as low as 473 K, the chain-growth probability was enhanced significantly, to

0.96. The conversion was still as high as 42.9% due to the smaller cobalt particle size and higher cobalt loading. The hydrocarbon distribution is displayed in Fig. 1. A very flat hydrocarbon distribution, in an anti-ASF distribution pattern, was obtained and waxy product selectivity was extremely high.

DISCUSSION

The prerequisite for an ASF polymerization theory is that desorbed C_{*n*}H_{2*n*} from the metal surface does not readorb onto the catalyst surface (1). The irregularly flat distribution of the hydrocarbons in 473 K clearly indicates that the ASF theory is only suitable for an ideal state. At low reaction temperatures here, the readsorption possibility of C_{*n*}H_{2*n*} was high even when supercritical *n*-pentane coexisted (13). These readorbed olefins initiated a new carbon chain-growth process, by consuming –CH₂–, to increase the formation rate of heavy hydrocarbons. Heavy olefins with a very low diffusion ability were ready to receive secondary hydrogenation to form heavy normal paraffins. At the present stage the present authors have no direct evidence to prove that olefin readsorption increases with decreasing temperature. From our previous report (13), the added olefin, such as 1-tetradecene or 1-hexadecene into supercritical-phase *n*-pentane, altered hydrocarbon distribution drastically, to a very flat pattern at 493 K. Furthermore, this phenomenon was more obvious when the amount of added olefin in the supercritical fluid was increased (19). A report from Kuipers *et al.* proved that the ratio of paraffin to olefin of carbon number *n* fraction had the relationship (20)

$$P_n/O_n \propto D_n^{-1} \exp(n\Delta G_1/RT),$$

where P_n is the amount of formed paraffin with carbon number *n*, O_n is the amount of formed olefin with carbon number *n*, D_n is the diffusion coefficient of hydrocarbon with carbon number *n*, *n* is the carbon number, and ΔG_1

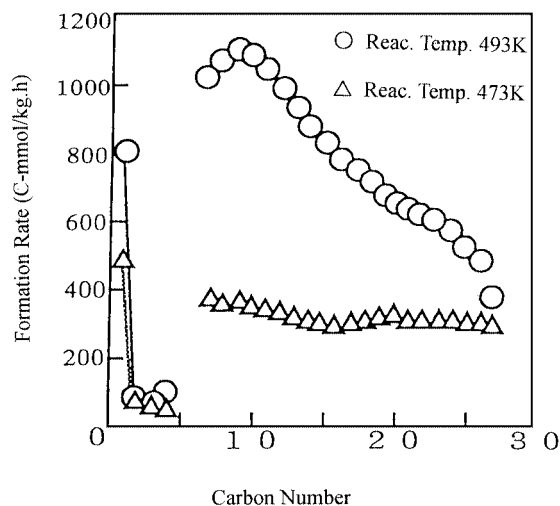


FIG. 1. Anti-ASF hydrocarbon distribution in FTS reactions with supercritical-phase *n*-pentane. Co/SiO₂ = 40/100 (wt.); P (total) = 45 bar; P (CO + H₂) = 10 bar; P (*n*-pentane) = 35 bar; CO/H₂ = 1/2; W/F (CO + H₂) = 9 g/mol h⁻¹.

is the change of free energy for the physisorption of a hydrocarbon, with carbon number 1 out of the wax onto the solid-to-wax interface and where $n\Delta G_1 = \Delta G_n$.

From this expression, it seems that when the temperature is lower, the readsorption probability of olefin increases remarkably. The readsorption possibility of olefins is remarkably lower for FTS at higher temperatures, leading to a classical ASF distribution pattern for the obtained hydrocarbons.

Iglesia *et al.* also proved that diffusion coefficient D_n obeyed the relationship (21)

$$D_n = D_0 \exp(-0.3n).$$

It is clear here that waxy olefin readsorbs onto the catalyst surface more quickly and it is believed that the diffusion coefficient decreases with a decrease in temperature (22).

It is also proved that little of the readsorbed olefin was hydrogenated secondly to form paraffin and that the main part initiated a new carbon chain propagation, resulting in the anti-ASF distribution (23).

It is well-known that generally methane selectivity is lower when chain-growth probability becomes higher. But in some cases methane selectivity exhibits irregular behavior, especially here where readsorption of olefin plays an important role in the carbon chain growth. A part of $-\text{CH}_2-$ is consumed in the additional chain growth initiated by the readsorbed olefins. But from the equilibrium between surface $-\text{CH}_2-$ concentrations and surface CO concentrations, CO conversion will be increased in some cases, if the coverage of waxy hydrocarbons is not too high. This will make methane selectivity higher, possibly. We proved that 1-olefin addition in supercritical fluid increased CO conversion but too high a content of the added 1-olefin in the supercritical fluid lowered CO conversion. Further, diene addition lowered CO conversion (13, 19). Higher coverage of olefin in the catalyst surface is an obstacle to the adsorption of CO. The surface coverage equilibrium among CO, $-\text{CH}_2-$, and adsorbed heavy hydrocarbon, as well as other factors, such as reaction temperature and length of the adsorbed hydrocarbon, determines the change trend of the CO conversion and methane selectivity, as opposed to the mechanism in a conventional, nonaddition reaction. Indeed methane selectivity in a supercritical-phase 473-K reaction was only 1% higher than that in a 483 K reaction for the catalyst calcined at 423 K shown in Table 2.

Due to the high activity of the Co/SiO₂ catalyst shown in Table 2, all three catalysts calcined at different temperatures exhibited the same CO conversion of 100% at 493 K.

In Table 2, for the catalyst calcined at 423 K, the reaction behavior of the gas-phase reaction at 473 K is also listed. Compared to that in the supercritical phase, CO conversion and methane selectivity were higher and chain-growth probability was lower. As the diffusion efficiency of syn-

gas in the gas phase was higher in the supercritical phase, CO conversion was higher in the gas-phase reaction. Introduction of supercritical fluid could promote heat transfer and prevent wax deposition as well as possible coke formation. Resultantly, methane formation was suppressed. Higher chain-growth probability is a characteristic feature of the supercritical-phase reaction, which was discussed in detail in the previous reports of the present authors (14, 15).

The chain-growth propagation is favored at lower temperatures. To obtain a high yield of wax, high CO conversion is necessary. To realize the high activity at low temperatures, effects from cobalt-loading amount and calcination temperature were studied. High CO conversion could realize high $-\text{CH}_2-$ concentration at the catalyst surface. More important, higher CO conversion increased the concentration of the formed heavier 1-olefins, and the latter adsorbed onto the catalyst more easily at low temperatures, such as 473 K. Based on this result, high CO conversion at a low temperature was fundamental to realizing anti-ASF distribution. The accompanying supercritical fluid was also critical to obtaining anti-ASF distribution, as it transported quickly the formed waxy hydrocarbons, mostly paraffin finally, out of the catalyst bed. As indicated in Table 2, using the same catalyst under the same reaction conditions, supercritical-phase reactions showed higher growth probability than did gas-phase reactions.

When the reaction was conducted at 473 K, the reaction temperature was only 3 K higher than the T_c of *n*-pentane. But we have proved that when the partial pressure of *n*-pentane in the reaction was higher than the P_c of *n*-pentane, the same reaction performance was available even when the reaction temperature was slightly lower than the T_c of *n*-pentane (24).

REFERENCES

1. Anderson, R. B., "The Fischer-Tropsch Synthesis." Academic Press, New York, 1984.
2. Sie, S. T., Senden, M. M. G., and van Wechem, H. M. H., *Catal. Today* **8**, 371 (1991).
3. Pichler, H., Schulz, H., and Kuhne, D., *Brennst. Chem.* **49**, 344 (1968).
4. Pichler, H., Schulz, H., and Elstner, M., *Brennst. Chem.* **48**, 3 (1967).
5. Bell, A. T., *Catal. Rev.-Sci. Eng.* **23**, 203 (1981).
6. Ekerdt, J. G., and Bell, A. T., *J. Catal.* **62**, 19 (1980).
7. Hall, W. K., Kokes, R. J., and Emmett, P. H., *J. Am. Chem. Soc.* **82**, 1027 (1960).
8. Novak, S., Madon, R. J., and Suhl, H., *J. Catal.* **77**, 141 (1982).
9. Iglesia, E., Reyes, S. C., Madon, R. J., and Soled, S. L., *Adv. Catal.* **39**, 221 (1993).
10. Madon, R. J., Reyes, S. C., and Iglesia, E., *J. Phys. Chem.* **95**, 7795 (1991).
11. Schulz, H., and Claeys, M., *Appl. Catal.* **186**, 71 (1990).
12. Iglesia, E., Soled, S. L., and Fiato, R. A., *J. Catal.* **137**, 212 (1992).
13. Fujimoto, K., Fan, L., and Yoshii, K., *Top. Catal.* **2**, 259 (1995).

14. Fan, L., and Fujimoto, K., *Appl. Catal.* **186**, 343 (1999).
15. Fan, L., Yokota, K., and Fujimoto, K., *AIChE J.* **38**, 1639 (1992).
16. Nijs, H. H., and Jacobs, P. A., *J. Catal.* **65**, 328 (1980).
17. Kellner, C. S., and Bell, A. T., *J. Catal.* **75**, 251 (1982).
18. Adachi, M., Yoshii, K., Han, Y., and Fujimoto, K., *Bull. Chem. Soc. Jpn.* **69**, 1509 (1996).
19. Yan, S., Fan, L., Zhang, Z., Zhou, J., and Fujimoto, K., *Appl. Catal. A* **171**, 247 (1998).
20. Kuipers, E. W., Vinkenburg, I. H., and Oosterbeek, H., *J. Catal.* **152**, 137 (1995).
21. Iglesia, E., Reyes, S. C., and Madon, R. J., *J. Catal.* **129**, 238 (1991).
22. Levenspiel, O., "Chemical Reaction Engineering," 2nd edition, Wiley, New York, 1972, p. 491.
23. Fan, L., Yan, S., Fujimoto, K., and Yoshii, K., *J. Chem. Eng. Jpn.* **30**, 923 (1997).
24. Yokota, K., Hanakata, Y., and Fujimoto, K., *Fuel*; **70**, 989 (1991).